Letters 31B, 297 (1970).
[55]D. D. Watson, private communication.
[56]B. W. Hooton, O. Hausser, F. Ingebretsen, and T. K. Alexander, Can. J. Phys. 48, 1259 (1970).
[57]O. Hausser, D. Pelte, T. K. Alexander, and H. C. Evans, Can. J. Phys. 47, 1065 (1969).
[58]F. Ingebretsen, T. K. Alexander, O. Hausser, and D. Pelte, Can. J. Phys. 47, 1295 (1969).
[59]L. K. ter Veld and T. W. van der Mark, Phys. Rev. 173, 1101 (1968).
[60]C. E. Moss, Nucl. Phys. A131, 235 (1969).
[61]H. D. Graber and G. I. Harris, Phys. Rev. 188, 1685 (1969).
[62]P. M. DeLucca, J. C. Lawson, and P. R. Chagnon, Bull. Am. Phys. Soc. 15, 566 (1970); and private communication.
[63]C. E. Moss, R. V. Poore, N. R. Roberson, and D. R. Tilley, Nucl. Phys. A144, 577 (1970).
[64]B. H. Wildenthal and E. Newman, Phys. Rev. 174, 1431 (1968.

PHYSICAL REVIEW C VOLUME 4, NUMBER 4 OCTOBER 1971

$E1$ and $M1$ Radiative Strength in ^{53}Cr, ^{57}Fe, and ^{61}Ni from Threshold Photoneutron Cross Sections*

H. E. Jackson and E. N. Strait†
Argonne National Laboratory, Argonne, Illinois 60439
(Received 5 May 1971)

The photoneutron cross sections for ^{53}Cr, ^{57}Fe, and ^{61}Ni have been measured near threshold with high resolution. Nuclear states of interest were excited by photon absorption from a bremsstrahlung beam whose end-point energy was sufficient only for neutron decay to the ground state of the daughter. Spins of resonances were assigned on the basis of angular distributions determined from the spectra for neutron emission at angles of 90 and 135°; the ground-state radiation widths $\Gamma_{\gamma 0}$ for most resonances were determined from the observed yields. Parity assignments were based on a comparison of data with total neutron cross sections of the daughter nuclei. The central feature of the results is an intense p-wave component whose integrated strength for all targets is greater than that of the s-wave component. In addition, an anomalous concentration of $M1$ strength is observed in an intense doublet with $J^\pi = \frac{3}{2}^-$ at $E_n = 230$ keV in the cross section for ^{57}Fe. The reduced widths for $E1$ and $M1$ radiation are consistent with the values $\bar{k}_{E1} = 0.0012$ and $\bar{k}_{M1} = 0.019$, respectively.

No evidence is found in the reactions ^{53}Cr(γ,n) and ^{57}Fe(γ,n) near threshold for doorway states which have been proposed in the literature. The data were also tested for a correlation between the reduced neutron width for s-wave resonances in each target and the corresponding ground-state radiation widths. In no case is there evidence for a significant correlation. Therefore the strong correlation reported between the reduced neutron widths and total radiation widths for s-wave resonances in even-even target nuclei in this mass region should not be attributed to the ground-state transition.

I. INTRODUCTION

One of the principal objectives in the study of γ-ray decay from individual highly excited nuclear states is observation of the influence of nuclear structure on the intensity of primary transitions. Among the nuclear-structure effects expected are rapid variations with excitation energy and atomic mass of the mean intensities for both electric and magnetic dipole transitions. The physical quantity which is expected to reflect these phenomena is the radiative strength function $\bar{\Gamma}/D$ for the appropriate multipole, where $\bar{\Gamma}$ is the average radiative width for transitions of a given multipolarity and D is the mean spacing of excited states whose spins and parities are such that these transitions are allowed. Because this parameter describes the average properties of radiative transitions, including any energy or mass dependence, experimental efforts have frequently focused on its measurement and comparison with various theoretical models.

Extensive experimental information is already available for electric dipole transitions. Although the small number of experimental samples still prevents decisive comparison of data with various predictions for mass dependence, the influence of the giant dipole resonance on $E1$ radiative strength has been observed[1] in several nuclei; specifically, the strength function varies more sharply with photon energy than would be expected from single-particle estimates. More detailed phenomena, such as the existence of relatively sharp variations in the strength of $E1$ transitions in the mass region $180 < A < 208$ and the energy region $E_\gamma \approx 5.5$ MeV,

are currently the subject of extensive investigation.[2]

By contrast, our understanding of the systematics of magnetic dipole transitions is still fragmentary. $M1$ transitions are characteristically weaker and more difficult to observe than $E1$. The accuracy of most experiments has been limited by the large statistical fluctuations known to characterize the distribution of partial radiation widths and the possibility of confusing transitions of different multipolarities because of inadequate knowledge of the spins and parities of the radiating states. Only for a few nuclei have observations been made for a significant sample of resonances with established spin and parity. The only conclusion clearly supported by existing data[3] is that the average $M1$ strength is strongly enhanced over the Weisskopf single-particle estimate and for a majority of nuclei is consistent with an average enhancement factor of ~15.

Neutron-capture studies have provided most of the data available for radiative transitions in the 7–11-MeV region. Recently, however, high-resolution studies of photoneutron spectra at threshold have become a promising source of information. Nuclear states of interest are excited by photon absorption from a bremsstrahlung beam whose endpoint energy is sufficient only for neutron decay to the ground state of the daughter nucleus, and are observed through their decay by neutron emission. The individual resonance yields are a measure of the radiative widths for ground-state-to-excited-state transitions in the parent nucleus. Although this technique was originally proposed and demonstrated as early as 1961,[4,5] only in recent years have improved experimental intensity and resolution permitted study[6,7] of a significant number of target nuclei. Because the (γ,n) reaction is very efficient in the sense that every interaction is the result of a transition between the ground state and an excited state in the parent, angular momentum can be assigned on the basis of photoneutron angular distributions even for relatively weakly excited levels. For many targets one can obtain an experimental sampling of a large number of resonances of a given spin and parity, a necessity for successful observation of photon strength functions.

The data presented here are the results of a series of threshold photoneutron measurements of ^{53}Cr, ^{57}Fe, and ^{61}Ni. These targets are of interest because they contain configurations near the $N = 28$ closed shells for either protons or neutrons. Possible enhancement of $M1$ transitions in mass regions near closed shells has been suggested by several authors.[8,9] In addition, these nuclei have several experimental advantages. Their low spin values and large expected mean radiation widths should result in observable intensities for both $E1$ and $M1$ photoexcitation of excited states. The possible angular distributions have easily recognized shapes characteristic of the spin sequences expected. In addition, detailed information is available from experiments with the inverse reactions in which the states observed in the photoneutron reaction are excited by neutron capture in the photoneutron daughter. The outstanding feature of the results is the exceptional strength of the p-wave resonances that dominate the photoneutron spectra. These resonances are excited by the absorption of magnetic dipole and possibly electric quadrupole radiation, and their unexpected intensity indicates that in the $A \approx 50$ mass region, $M1$ and $E1$ transitions are of comparable strength. The assigned spins and parities exhaust almost all the radiative strength observed in each component of the resonance structure, and the values obtained for both $E1$ and $M1$ photon strength functions are much more precise than had been available earlier.

II. EXPERIMENTAL TECHNIQUE

The basic idea of the threshold photoneutron technique is illustrated schematically in Fig. 1, where the parameters for a ^{53}Cr target are presented as an illustrative example. The key to the method is the use of an intense bremsstrahlung beam of very precisely determined maximum energy. With this energy definition, excitation by photon absorption can be limited to a small band of excited levels just above the neutron binding energy. Subsequent decay of these states must be either by neutron emission to the ground state of the daughter or by radiative decay to lower states of the target.

In the thin-target approximation, which is adequate for the weak absorption characteristic of these experiments, the yield in the neutron

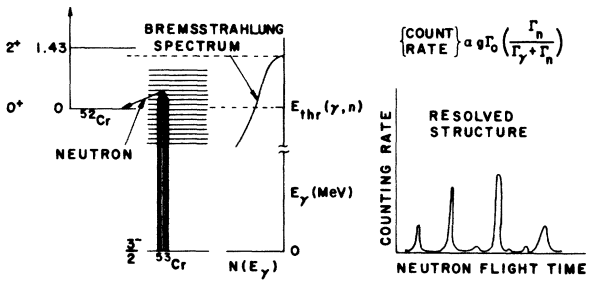

FIG. 1. Schematic representation of the principle of the threshold photoneutron experiment with a ^{53}Cr target. A state in the compound system cannot be excited if it lies above the energy limit set by the end point of the bremsstrahlung spectrum. For the case shown here, neutron emission is possible only to the ground state of ^{52}Cr.

channel for a given level is given by

$$Y(\lambda) = 2\pi^2\lambda^2 g\Gamma_{\gamma 0}\Gamma_n/\Gamma\,, \tag{1}$$

where $g = \frac{1}{2}(2J+1)/(2I+1)$ is the statistical factor in which I and J are the spins of the target and excited state, respectively, λ is the reduced photon wavelength, $\Gamma_{\gamma 0}$ is the radiative width for direct decay to the ground state of the target, and Γ_n and Γ are the neutron and total resonance widths, respectively. Observation of the resulting neutron time-of-flight spectrum with established time-of-flight techniques reveals a structure of individual resonances, each with a neutron energy uniquely related to that of the excited state and with an integrated intensity given by Eq. (1). The angular distribution of photoneutrons is expected to be isotropic only for resonances with specific values of J.

Spin and parity considerations for ^{53}Cr are illustrated in Fig. 2. Absorption of electric dipole radiation can lead to excitation of even-parity states with spins $\frac{1}{2}$, $\frac{3}{2}$, and $\frac{5}{2}$. The subsequent decay of $\frac{1}{2}$ states will be, in lowest order, by emission of s-wave neutrons, and the decay of $\frac{3}{2}$ and $\frac{5}{2}$ states will be by emission of d-wave neutrons. Absorption of magnetic dipole radiation will excite states of the same spin values but odd parity. The resonances with spin $\frac{1}{2}^-$ and $\frac{3}{2}^-$ will decay by emitting p-wave neutrons and $\frac{5}{2}^-$ levels by emitting f-wave neutrons. Each of the possible spin sequences will have a characteristic angular distribution.[10] Only the $\frac{3}{2} \to \frac{1}{2} \to 0$ sequence will be isotropic. The angular distributions expected for each sequence have been calculated under the assumption that only dipole absorption occurs. The results indicate that comparison of intensities at 90 and 135° should give easily recognized unique ratios for the possible values of the resonance spin for each of the targets studied here. The expected values for the 90 to 135° ratio for ^{53}Cr$(\gamma, n)^{52}$Cr are shown in the table at the bottom of Fig. 2.

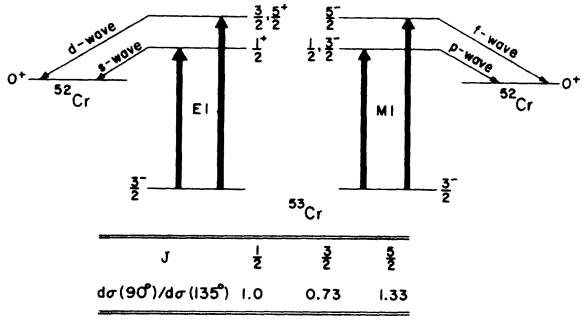

FIG. 2. Excitation and decay diagram for the reaction ^{53}Cr(γ, n). Excitation is assumed to result from dipole photon absorption, and decay is assumed to be by neutron emission to the ground state of ^{52}Cr.

The bremsstrahlung source and experimental apparatus are shown in Fig. 3, a schematic diagram of the Argonne threshold photoneutron facility. The linear accelerator is a two-section L-band machine[11] which can accelerate electrons to energies of 4–22 MeV when operated in the short-pulse mode. For the photoneutron experiments the electron pulse has a 6-nsec duration, a repetition rate of 720 sec^{-1}, and peak currents of 10–20 A depending on operating conditions. The electron beam from the linac passes through a 90° analyzing magnet and emerges with an energy spread less than 300 keV. The beam is then focused, restored to its original direction, and allowed to strike a thin radiator (the converter in Fig. 3). To be suitable for the radiator, a material should have a neutron threshold sufficiently high that no neutron background can be generated by it. For these studies, a 20-mm Ag foil was used. The resulting bremsstrahlung passes through a block of aluminum (which stops the electrons) and irradiates the target in which the (γ, n) reaction occurs. The photoneutrons are observed along flight tubes placed at 90, 135, and 155° to the direction of the bremsstrahlung beam. They are detected in a bank of neutron detectors at the end of each flight tube, and their energies are determined by their flight times. The detectors, six in each bank, are conventional ^{6}Li glass scintillators 12.5 cm in diameter and $\frac{3}{8}$ in. thick. To reduce the intensity of low-energy bremsstrahlung scattered by the target in the direction of the detectors, filters of bismuth or

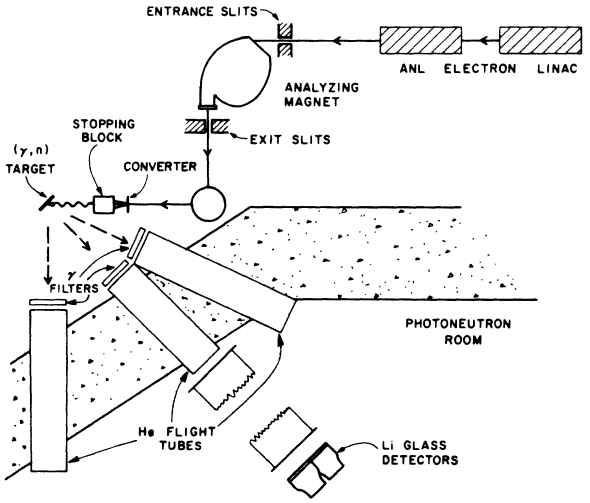

FIG. 3. Threshold photoneutron facility. The Argonne National Laboratory linac is located in a vault separated from the photoneutron room by a shielding wall 7 ft thick. Both rooms are below ground level. The beam diameter at the converter is 1 cm; the distance from converter to target is 13.7 cm. The flight path at each available angle varies from 5 to 18 m.

lead 2 cm thick are placed across the entrances to the flight tubes. Without these filters the 6-nsec burst of scattered bremsstrahlung produces undesirable afterglow in the scintillators and overloading of the photomultipliers. In addition, two dynodes on each detector photomultiplier are gated "off" until about 300 nsec after the burst.

Time analysis of neutron events is carried out with a conventional time-to-amplitude converter system in which the timing cycle is started by the charge pulse generated in the aluminum stopping block when the electron pulse arrives. The aluminum block is also used as a Faraday cup to integrate the total electron charge absorbed in producing bremsstrahlung. The intensities of all neutron spectra are measured in neutrons per coulomb of integrated charge.

The most serious limitation on the precision of threshold photoneutron measurements is the accuracy of any absolute normalization. Uncertainties in the effective photon flux as a function of energy and of angle with respect to the electron beam arise from the difficulty in calculating the expected spectrum shape in the high-energy region near the short-wavelength limit of the spectrum. In place of the usual thin-target approximation, one must carry out a thick-target calculation in which the effects of multiple scattering and energy loss are included. Any inadequacies in the thin-target spectrum, such as those discussed by Berger and Seltzer,[12] will be perpetuated in such a calculation. To date such thick-target spectra have been confirmed[13] with only limited precision. The problem is compounded by the very sharp angular dependence in the intensity of bremsstrahlung. At 9.1 MeV the half-width of the photon flux as a function of opening angle is only 9.5° for a 20-mil silver radiator. Consequently the bremsstrahlung intensity at the (γ, n) sample will be a sensitive function of beam location and extent, particularly for the short radiator-to-sample distance used in the present measurements. In our judgment, these facts preclude an accurate calculation of the absolute photon flux per unit charge at the present time.

Instead, we adopted an alternative approach of using the 40.7-keV resonance in the reaction ^{208}Pb(γ, n) as a primary standard. From studies[14,15] of neutron capture in ^{207}Pb, the value $g\Gamma_{\gamma 0} = 3.18 \pm 0.61$ eV has been established for this level. Absolute normalization of photoneutron spectra can be accomplished by calibrating every photoneutron run with a short run with a Pb target whose cross-sectional dimensions are identical to those of the sample being studied. The yield for the lead resonance determines the number of counts per coulomb for a given value of $Y(\chi)$. Variations in the effective photon flux as a result of differences in the (γ, n) threshold require only small corrections, and these involve only relative intensities in the spectrum of the incident flux. Because all results are relative to a single standard, any future increase in the precision of the standard can be applied readily to all measurements.

Because the Pb spectrum is used to normalize each sample run, only relative detector efficiencies are necessary in calculating resonance widths for all levels observed. The ^{6}Li(n, α) cross sections used to estimate the relative efficiencies were taken from the tabulated evaluated data contained in the ENDF/B[16] file. However, as recent discussions indicate,[17] the available data on all ^{6}Li cross sections are consistent only within limited precision and suggest that the Li(n, α) cross sections may contain substantial errors. To assess the importance of multiple scattering in the Li(n, α) reaction, Monte Carlo calculations were carried out for the glass scintillators used in this experiment. The results show that multiple-scattering effects enhance detection efficiency by as much as 20–30%. These same effects may be responsible in part for the discrepancies in presently accepted cross sections, i.e., the effects of multiple scattering may not have been eliminated from the cross sections used to obtain the evaluated data set. If this is true, the Monte Carlo treatment based on evaluated cross sections would give estimates of multiple scattering which are much too large. In view of this, the Monte Carlo results were used only as a guide to the accuracy with which *relative* detector efficiencies could be calculated, and the actual relative values were determined from the tabulated ^{6}Li(n, α) cross section without taking any account of multiple scattering. The uncertainty due to multiple-scattering effects is largest, about 8%, in the energy region from 30 to 120 keV.

III. DATA

For each target, observations were made at 90 and 135° to the electron beam with flight paths of 9 m. The over-all time-of-flight resolution was 1 nsec/m for these spectra. In favorable cases, measurements were also made at shorter flight paths. The duration of each individual run was approximately 24 h. In all cases the end point of the photon spectrum was chosen so that the only neutron channel open to continuum states excited by photon absorption is decay to the ground state of the daughter nucleus. The most prominent feature of the spectra is the exceptional strength of p-wave resonances. In all cases the integrated yield of this component is at least as great as that of s-wave levels. The results for each target are discussed below individually.

^{53}Cr

A 64.4-g target of Cr_2O_3 enriched to 96% in ^{53}Cr was irradiated by a pulsed bremsstrahlung beam with an end-point energy of 9.1 MeV. Data taken at 135° are shown in Fig. 4. The broad peak in the resonance structure observed in the region of channel 1200 is caused by increased detection efficiency in the neighborhood of the 255-keV resonance in the $^6Li(n, \alpha)T$ reaction. Observed resonance energies agree very well with those calculated from the total capture cross sections[18, 19] of ^{52}Cr upon correcting the latter for recoil effects. However, not all resonances seen in capture in ^{52}Cr will be observed in $^{53}Cr(\gamma, n)$ because the photoneutron yields are proportional to the ground-state radiation width, a quantity which fluctuates greatly from resonance to resonance.

To determine the resonance spins from photoneutron angular distributions, the s-wave resonances in the (γ, n) spectra were located from the measured total neutron cross sections of ^{52}Cr, and data for 90 and 135° were normalized so that the relative yields gave isotropy for the s-wave resonance at 226 keV. The ratio of the 90 to the 135° yield was then calculated for all other neutron groups. The results are listed in Table I for those resonances for which definite assignments could be made. The spin assignments shown are based on the observed intensity ratio, which is expected

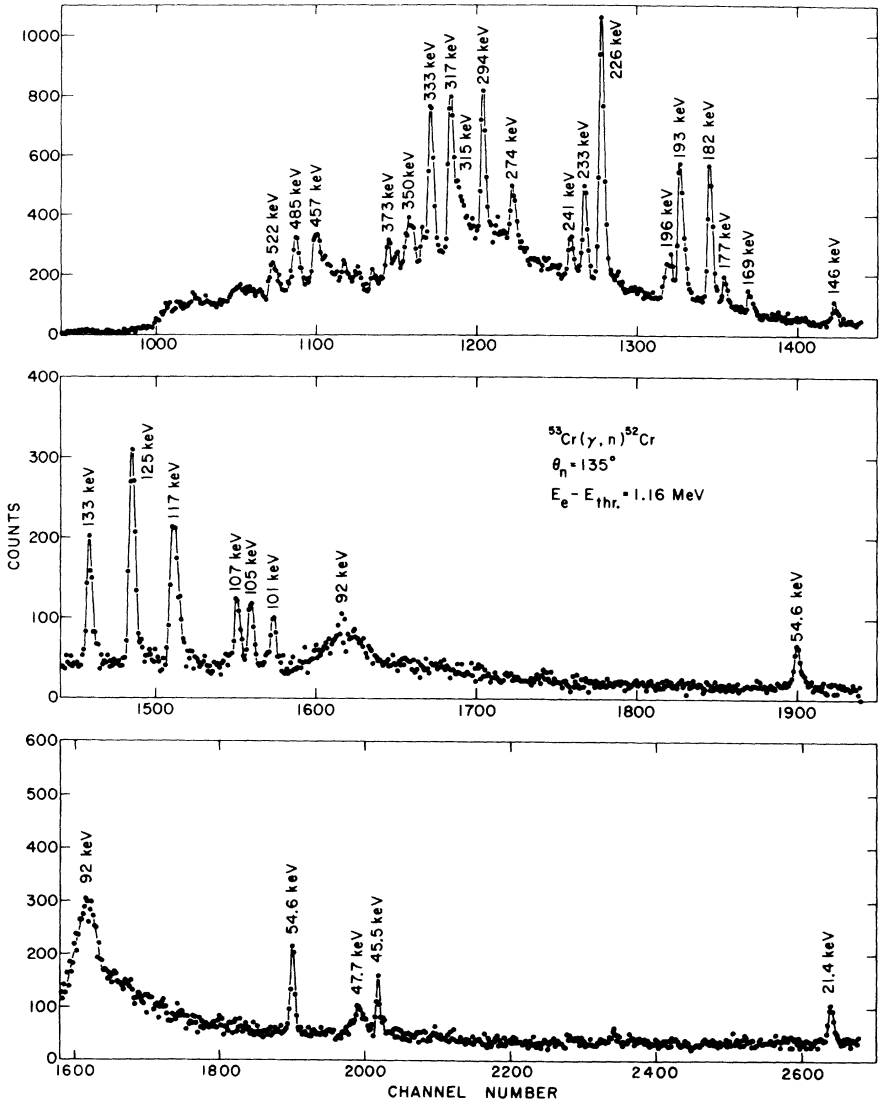

FIG. 4. Photoneutron time-of-flight spectrum for $^{53}Cr(\gamma, n)$. The flight path was 9 m. In the section for channels 1600 to 2700, each point represents the sum of two adjacent channels.

to be $I(90°)/I(135°) = 1.0$, 0.73, and 1.33 for total angular momentum $\frac{1}{2}$, $\frac{3}{2}$, and $\frac{5}{2}$, respectively, if only dipole absorption of photons occurs. One cannot *a priori* rule out excitation of the $\frac{1}{2}^-$ and $\frac{3}{2}^-$ levels by a mixture of $M1$ and $E2$ radiation, but the values observed for the ratio $I(90°)/I(135°)$ indicate that any $E2$ component is very weak. To emphasize this point a histogram of the values of $I(90°)/I(135°)$ for the non-s-wave levels observed in ^{53}Cr is presented in Fig. 5. This ratio is extremely sensitive to any $E2$ admixture.[10] Depending upon its phase relative to the $M1$ component, a 1% $E2$ component would increase or decrease the expected ratio by as much as 0.09. The clear grouping of the observed values in Fig. 5 around the ratios appropriate to pure $M1$ transitions is evidence that the probability of error is small in assigning spins on the basis of pure dipole transitions. In fact the only possible evidence for the presence of a very weak $E2$ component is the somewhat low value of the ratio observed for the 101- and 125-keV resonances.

The data of Table I and Fig. 5 also contain strong evidence for the absence of resonances which decay by emission of d-wave neutrons. No values of the intensity ratio corresponding to resonances with $J = \frac{5}{2}$ are observed nor is a corresponding group present in Fig. 5. Such levels would decay only by d-wave emission to the ground state of ^{52}Cr. Assuming that there is no strong spin dependence in the d-wave average reduced neutron widths for $j = \frac{3}{2}$ and $\frac{5}{2}$, we can interpret the absence of $j = \frac{5}{2}$ resonances as indicating that there is no d-wave emission from either spin state in the region studied. This conclusion is consistent with the implications of the data on the total neutron cross section of ^{52}Cr. The yield of photoneutrons is proportional to $\Gamma_n\Gamma_{\gamma 0}/(\Gamma_n+\Gamma_\gamma)$. The inhibition of d-wave emission can be attributed to small values of the d-wave neutron width which result from the low transmission coefficients for d-wave neutrons in the energy range of this experiment. To test this explanation, we have taken the observed spacings of d-wave levels from the total cross-section results of Newson *et al.*[20] and used them together with the d-wave transmission coefficients calculated from an optical-model potential to obtain an estimate of the average neutron widths for d waves. Though admittedly crude and sensitive to precise features of the potential used, the results do show that for d waves $\overline{\Gamma}_n$ is smaller than the radiative width and consequently the average branching ratio for decay by d-wave neutron emission is less than 1. For example, at 100 keV $\overline{\Gamma}_n/(\overline{\Gamma}_n+\Gamma_\gamma)\approx 0.2$ if we use the value of $\Gamma_\gamma = 4$ eV. Thus the absence of d-wave resonances is not unexpected. We will assume in all the discussion which follows that all levels which do not correlate with known s-wave levels observed in the inverse reaction decay by p-wave neutron emission. The observations above indicate that the probability of an incorrect parity assignment resulting from this assumption is small.

In order to emphasize the strength of the various components in the resonance structure of the photoneutron spectra, the data for the resonance parameters (Table II) are organized according to resonance spin and parity. The integrated yield of p-wave levels, which is proportional to $\sum g\Gamma_{\gamma 0}\Gamma_n/\Gamma$ is more than twice that for s-wave levels. For $\frac{1}{2}^-$

TABLE I. Angular momentum assignments for resonances in the reaction ^{53}Cr(γ, n). Excitation of levels is assumed to take place only by absorption of dipole radiation.

$E_n(\gamma,n)$ (keV)	$\frac{d\sigma(90°)/d\Omega}{d\sigma(135°)/d\Omega}$	J^π	$E_n(\gamma,n)$ (keV)	$\frac{d\sigma(90°)/d\Omega}{d\sigma(135°)/d\Omega}$	J^π
47.7	s wave	$\frac{1}{2}^+$	196	0.78 ± 0.08	$\frac{3}{2}^-$
92	s wave	$\frac{1}{2}^+$	226	s wave	$\frac{1}{2}^+$
101	0.54 ± 0.06	$\frac{3}{2}^-$	233	1.10 ± 0.06	$\frac{1}{2}^-$
105	0.69 ± 0.06	$\frac{3}{2}^-$	241	0.72 ± 0.08	$\frac{3}{2}^-$
107	0.70 ± 0.06	$\frac{3}{2}^-$	274	0.66 ± 0.07	$\frac{3}{2}^-$
117	s wave	$\frac{1}{2}^+$	294	1.09 ± 0.04	$\frac{1}{2}^-$
125	0.53 ± 0.03	$\frac{3}{2}^-$	315	s wave	$\frac{1}{2}^+$
133	0.66 ± 0.04	$\frac{3}{2}^-$	317	0.71 ± 0.03	$\frac{3}{2}^-$
146	1.01 ± 0.10	$\frac{1}{2}^-$	333	1.01 ± 0.04	$\frac{1}{2}^-$
182	1.15 ± 0.03	$\frac{1}{2}^-$	350	0.68 ± 0.06	$\frac{3}{2}^-$
193	1.10 ± 0.03	$\frac{1}{2}^-$	373	1.06 ± 0.11	$\frac{1}{2}^-$

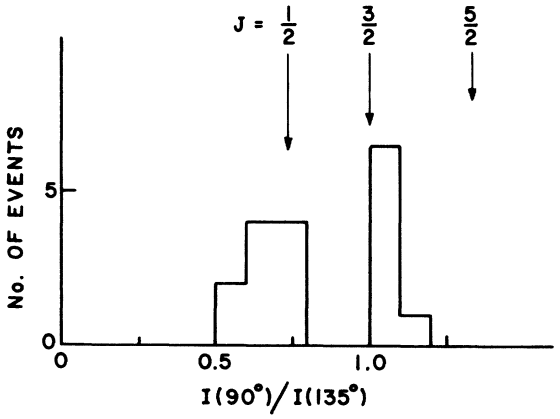

FIG. 5. Histogram of $I(90°)/I(135°)$ the ratio of the photoneutron intensity at emission angles of 90 and 135° to the incident beam in the reaction ^{53}Cr$(\gamma, n)^{52}$Cr. The arrows indicate the values of the ratio expected for each resonance spin if the levels are excited by pure dipole photon absorption.

and $\frac{3}{2}^-$ levels, $\sum g\Gamma_{\gamma 0}\Gamma_n/\Gamma = 2.13$ eV, as opposed to $\sum g\Gamma_{\gamma 0}\Gamma_n/\Gamma = 0.97$ for $j = \frac{1}{2}^+$ levels. The observed total strength for all p-wave levels is $\sum\Gamma_{\gamma 0}\Gamma_n/\Gamma = 6.8$ eV. Since a Weisskopf unit[21] is 11 eV, the total $M1$ strength is at least 0.6 of a Weisskopf unit.

^{57}Fe

A ^{57}Fe target consisting of 39.7 g of Fe_2O_3 enriched to 90.4% in ^{57}Fe was irradiated by a bremsstrahlung beam with an end-point energy of 8.45 MeV. The data obtained along the 90° beam line are shown in Fig. 6. The energies observed for the various neutron groups are in excellent agreement with values calculated from data on total[19] and capture[22] cross sections for ^{56}Fe. Calculated and observed energies are listed in Table III. Because $J^\pi = \frac{1}{2}^-$ for the ground state of ^{57}Fe, absorption of dipole photons can excite only levels with $J = \frac{1}{2}$ and $\frac{3}{2}$. For the spin sequence $\frac{1}{2} \to \frac{1}{2} \to 0$ the angular distribution will be isotropic, while for $\frac{1}{2} \to \frac{3}{2} \to 0$ the ratio will be $I(90°)/I(135°) = 1.43$ if only $M1$ absorption is considered. The data for 90 and 135° were normalized so that the relative yields gave isotropy for the strong s-wave level at 212 keV and the corresponding ratio was then calculated for the other resonances. In Table IV, assign-

TABLE II. Energies and parameters for resonances in the reaction ^{53}Cr(γ, n). The ±20% error in the quantity $\Gamma_{\gamma 0}\Gamma_n/\Gamma$ for all resonances is due mainly to the uncertainty in the absolute normalization of the data. The energies given in column 2 are calculated from those of column 1 by applying a correction for recoil effects. For unassigned levels, column 4 gives $g\Gamma_{\gamma 0}\Gamma_n/\Gamma$.

$E_n(n,\gamma)$ References 18, 19 (keV)	$E_n(\gamma,n)$ at $\theta = 135°$ Calc. (keV)	Obs. (keV)	$\Gamma_{\gamma 0}\Gamma_n/\Gamma$ (eV)
	$J = \frac{1}{2}^+$		
50.2 ± 0.3	47.3	47.7	0.179
97.1 ± 0.8	92.0	92.0	1.275
123.2 ± 1.0	117	117	0.930
141.4 ± 1.2	134	...	...
239.4 ± 2.2	228	226	1.315
285.4 ± 2.8	272	...	...
331.1 ± 3.5	316	315	0.184
		Total	3.884
	$J = \frac{1}{2}^-$		
155 ± 1.2	147	146	0.234
...	...	182	1.210
...	...	193	1.137
...	...	233	0.409
...	...	294	0.748
...	...	333	1.324
		Total	5.062
	$J = \frac{3}{2}^-$		
107 ± 0.8	101	101	0.075
111 ± 0.9	105	105	0.102
113 ± 0.9	107	107	0.143
132 ± 0.9	125	125	0.256
...	...	133	0.193
...	...	196	0.151
...	...	241	0.069
...	...	274	0.077
...	...	317	0.395
...	...	350	0.249
		Total	1.710
	Unassigned levels		
22.9 ± 1.0	21.3	21.4	0.026
48.3 ± 0.21	45.4	45.5	0.009
57.8 ± 0.28	54.5	54.6	0.046
...	...	175	0.046
		Total	0.127

TABLE III. Energies and parameters for resonances in the reaction ^{57}Fe(γ, n). The ±20% error in the quantity $\Gamma_{\gamma 0}\Gamma_n/\Gamma$ for all resonances is due mainly to the uncertainty in the absolute normalization of the data. The energies given in column 2 are calculated from those of column 1 by applying a correction for recoil effects. For unassigned levels, column 4 gives $g\Gamma_{\gamma 0}\Gamma_n/\Gamma$.

$E_n(n,\gamma)$ References 19, 22 (keV)	$E_n(\gamma,n)$ at $\theta = 90°$ Calc. (keV)	Obs. (keV)	$\Gamma_{\gamma 0}\Gamma_n/\Gamma$ (eV)
	$J = \frac{1}{2}^+$		
27.9	26.9	26.7	0.112
74	71.4	70.2	0.082
83.7	80.8	...	...
123.5	119.2	118.4	0.119
130	125.5	125.1	0.105
141	136	136	0.068
169	163	163	0.066
188	181	181	0.423
220	212	212	0.683
		Total	1.658
	$J = \frac{1}{2}^-$		
34.1	32.9	32.9	0.180
59	56.9	56.9	0.221
...	...	216	0.130
...	...	278	0.208
		Total	0.739
	$J = \frac{3}{2}^-$		
...	...	224	0.364
...	...	235	0.382
...	...	270	0.090
		Total	0.836
	Unassigned levels		
...	...	92.6	0.045
...	...	98.7	0.042
...	...	167	0.032
...	...	247	0.030
...	...	260	0.046
		Total	0.195

ments are given for all levels with sufficient yield to calculate the 90°/135° ratio with significant precision. The criterion for assignment of J for all targets was that the value assigned to a level must be at least 10 times as probable for the assigned value as for the other choice.

Table III lists the resonance parameters and compares calculated and observed resonance energies for each group of spins and parities. From the extensive data available for s-wave resonances in the total cross section of ^{56}Fe, a complete list of expected s-wave levels can be obtained. A measurable yield in the (γ, n) spectrum was observed for all but one known s-wave resonance. This observation suggests that if the observed population is governed by the usual Porter-Thomas statistics with an average ground-state width which satisfies the condition $g\Gamma_{\gamma 0} \gtrsim 0.05$ eV, then the sensitivity of the present experiment is adequate for observing the integrated strength of all levels that have a given spin and parity.

The distribution of radiative strength among p-wave levels is not consistent with a Porter-Thomas distribution of ground-state widths, and the assignments for $J = \frac{3}{2}^-$ suggest a strong concentration of $M1$ radiative strength in two resonances. Only three resonances with $J = \frac{3}{2}^-$ are observed, including the very intense doublet at 224 and 235 keV. However, other data indicate that a much larger number of p-wave resonances were undetected. In the capture cross section of ^{56}Fe, 16 presumed p-wave levels absent in this measurement were found below 130 keV. The mean value of $g\Gamma_{\gamma 0}$ resulting from the doublet alone is sufficiently high to guarantee that a substantially larger number of levels should have been observed if they were drawn from a Porter-Thomas distribution. Under the normal statistical assumption that the level density ρ is proportional to $(2J+1)$, the results for s-wave levels would imply that 30 resonances with $J = \frac{3}{2}^-$ should be in the energy region studied. The hypothesis that the observed concentration of strength results simply from a random fluctuation in an ordinary population of p-wave levels which

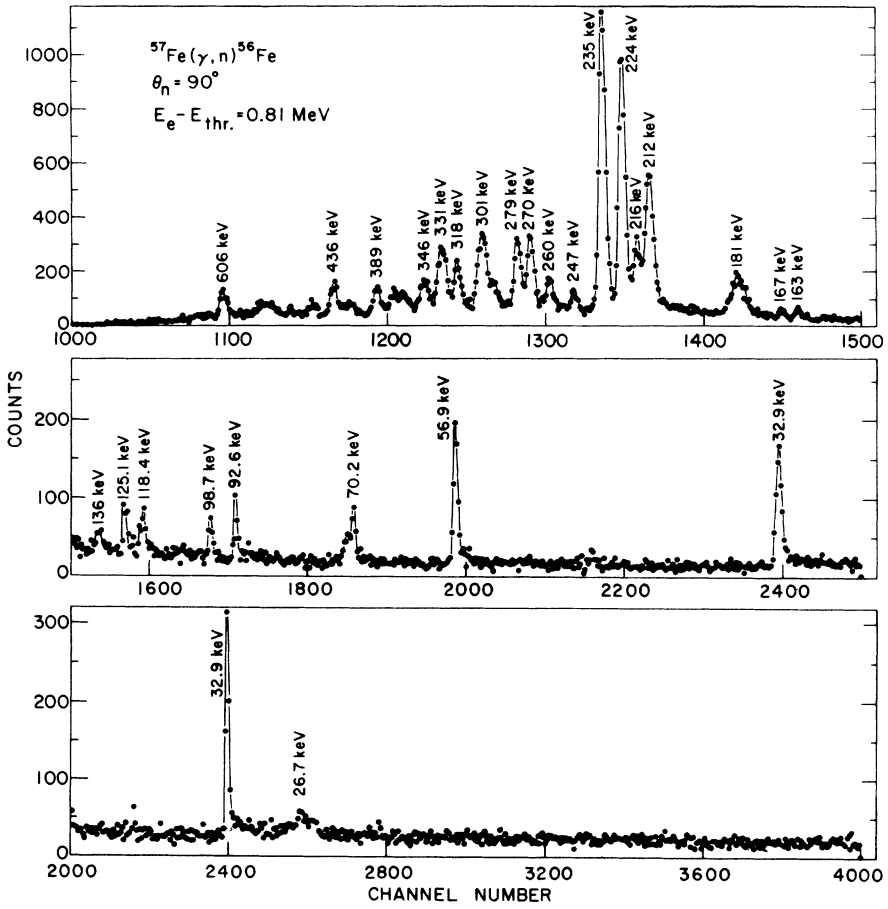

FIG. 6. Photoneutron time-of-flight spectrum for ^{57}Fe(γ, n). The flight path was 9 m. Each point in the center section represents the sum of two adjacent channels; in the lower section they represent sums of four adjacent channels.

are subject to the usual level-spacing and ground-state width statistics can be tested by determining the probability of obtaining a doublet whose individual widths are equal to or greater than the observed values. This probability was calculated under the assumptions that: (1) the radiation widths are drawn from a Porter-Thomas distribution, (2) resonance energies and widths are statistically independent, (3) $\rho \propto (2J+1)$, and (4) the radiative strength for $J = \frac{3}{2}^-$ resonances can be estimated by summing the widths of the assigned $\frac{3}{2}^-$ resonances and those of the observed but unassigned levels. The resulting $\overline{\Gamma}_{\gamma 0}$ assuming a total of 30 levels is less than 0.09 that of the weaker member of the doublet. The probability of such a distribution of strength is less than 10^{-4}. In view of this result, explanation of the observed concentration of radiative strength as a fluctuation in a Porter-Thomas distribution of levels appears untenable.

^{61}Ni

Photoneutron spectra resulting from irradiation of a ^{61}Ni target with bremsstrahlung, whose end point is 8.9 MeV, are shown in Fig. 7. The angle of observation is 90°. The target was a 32-g sample of nickel powder enriched to 92.4% in ^{61}Ni. Extensive measurements[18] of capture and total neutron cross sections for ^{60}Ni were reported recently. The very broad photoneutron peak at 11.6 keV agrees very well in energy and width with the parameters observed for the s-wave resonance in these data at 12.47 keV.

TABLE IV. Angular momentum assignments for resonances in the reaction ^{57}Fe(γ, n).

$E_n(\gamma, n)$ (keV)	$\frac{d\sigma(90°)/d\Omega}{d\sigma(135°)/d\Omega}$	J^π	$E_n(\gamma, n)$ (keV)	$\frac{d\sigma(90°)/d\Omega}{d\sigma(135°)/d\Omega}$	J^π
26.7	s wave	$\frac{1}{2}^+$	181	s wave	$\frac{1}{2}^+$
32.9	1.10 ± 0.08	$\frac{1}{2}^-$	212	s wave	$\frac{1}{2}^+$
56.9	1.08 ± 0.09	$\frac{1}{2}^-$	216	0.90 ± 0.10	$\frac{1}{2}^-$
70.2	s wave, other	$\frac{1}{2}^+$, ?	224	1.32 ± 0.04	$\frac{3}{2}^-$
118.4	s wave	$\frac{1}{2}^+$	235	1.43 ± 0.04	$\frac{3}{2}^-$
125.1	s wave	$\frac{1}{2}^+$	270	1.36 ± 0.09	$\frac{3}{2}^-$
136.	s wave	$\frac{1}{2}^+$	278	0.99 ± 0.07	$\frac{1}{2}^-$
163.	s wave	$\frac{1}{2}^+$			

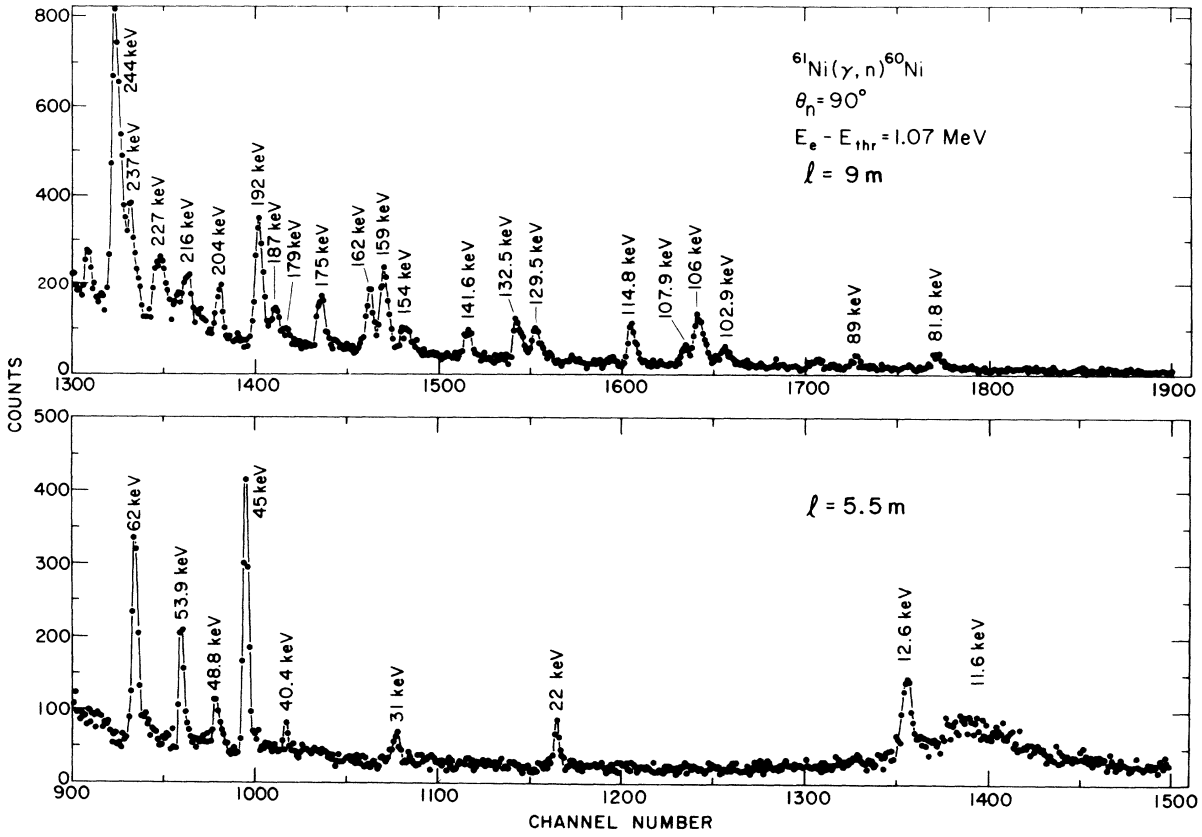

FIG. 7. Photoneutron time-of-flight spectrum for ^{61}Ni(γ, n). The upper section was taken with a flight path of 9 m, the lower section with a flight path of 5.5 m.

The angular momentum assignments for observed levels are listed in Table V. Normalization was more difficult for the Ni runs at 90 and 135° because the cross section of the Bi beam filter has a resonance near 11.6 keV, the energy of the only prominent s-wave level. To avoid the effects of resonances in the neutron cross sections of the beam filters, separate runs were made with Bi and Pb filters. The lower spectrum of Fig. 7 was taken with a Pb filter and a flight path of 5.5 m. The data for the two angles at 5.5 m were normalized to give isotropy for the 11.6-keV resonance. The higher energy levels were assigned from the data at the longer flight path; these runs were normalized from the observed intensities of s-wave levels in the Pb calibration runs. The angular dependences of the yields for the resonances at 8 and 53.9 keV were observed in both sets of data, and the results for the two sets, which were in agreement, are shown in Table V. Resonance parameters obtained from these spectra are given in Table VI.

IV. DISCUSSION

In the photoneutron experiments, the quantity measured for each resonance is $\Gamma_{\gamma 0}\Gamma_n/\Gamma$. The evidence from measurements of neutron capture and total cross sections of each of the daughter nuclei indicates that $\Gamma_n/\Gamma \approx 1$ is a good approximation for all the s-wave levels observed in this experiment. The parameters for p-wave levels must be considered in closer detail. The capture-cross-section results for ^{52}Cr, ^{56}Fe, and ^{60}Ni give values for $g(n,\gamma)\Gamma_\gamma\Gamma_n/\Gamma$. The total radiation width is not expected to fluctuate greatly from resonance to resonance. Consequently, if $\Gamma_n/\Gamma = 1$ is a valid assumption, the observed values of $g\Gamma_\gamma\Gamma_n/\Gamma$ will cluster around two characteristic values of $g(n,\gamma)\Gamma_\gamma$, the values for each of the two possible choices of resonance spin. On the other hand if $\Gamma_n/\Gamma \ll 1$, much smaller values would be observed. The data avail-

TABLE V. Angular momentum assignments for resonances in the reaction ^{61}Ni(γ, n).

$E_n(\gamma,n)$ (keV)	$\frac{d\sigma(90°)/d\Omega}{d\sigma(135°)/d\Omega}$	J^π	$E_n(\gamma,n)$ (keV)	$\frac{d\sigma(90°)/d\Omega}{d\sigma(135°)/d\Omega}$	J^π
11.6	s wave	$\frac{1}{2}^+$	102.9	s wave	$\frac{1}{2}^+$
12.6	1.15 ± 0.15	$\frac{1}{2}^-$	106.0	1.05 ± 0.07	$\frac{1}{2}^-$
22.0	0.59 ± 0.10	$\frac{3}{2}^-$	114.8	0.61 ± 0.05	$\frac{3}{2}^-$
31.0	0.56 ± 0.12	$\frac{3}{2}^-$	129.5	0.95 ± 0.09	$\frac{1}{2}^-$
40.4	s wave	$\frac{1}{2}^+$	132.5	0.91 ± 0.08	$(\frac{1}{2})^-$
45.0	1.13 ± 0.07	$\frac{1}{2}^-$	141.6	1.28 ± 0.19	$\frac{1}{2}^-$
48.8	0.64 ± 0.10	$\frac{3}{2}^-$	154.0	s wave	$\frac{1}{2}^+$
	0.49 ± 0.07		159.0	1.24 ± 0.08	$\frac{1}{2}^-$
53.9	0.97 ± 0.11	$\frac{1}{2}^-$	162.0	0.72 ± 0.06	$\frac{3}{2}^-$
	1.10 ± 0.12		179.0	s wave	$\frac{1}{2}^+$
62.0	0.68 ± 0.04	$\frac{3}{2}^-$	187	0.62 ± 0.05	$\frac{3}{2}^-$
	0.80 ± 0.05		192	s wave	$\frac{1}{2}^+$
81.8	0.61 ± 0.09	$\frac{3}{2}^-$			
92.6	s wave	$\frac{1}{2}^+$			

TABLE VI. Energies and parameters for resonances in the reaction ^{61}Ni(γ, n). The ±20% error in the quantity $\Gamma_{\gamma 0}\Gamma_n/\Gamma$ for all resonances is due mainly to the uncertainty in the absolute normalization of the data. The energies given in column 2 are calculated from those of column 1 by applying a correction for recoil effects. For unassigned levels, column 4 gives $g\Gamma_{\gamma 0}\Gamma_n/\Gamma$.

$E_n(n,\gamma)$ Reference 18 (keV)	$E_n(\gamma,n)$ at $\theta = 90°$ Calc. (keV)	Obs. (keV)	$\Gamma_{\gamma 0}\Gamma_n/\Gamma$ (eV)
	$J = \frac{1}{2}^+$		
12.47	11.64	11.6	0.367
28.64	27.00	···	···
43.08	40.86	40.4	0.018
65.13	62.04	···	···
86.8	82.77	···	···
98.1 ± 0.7	93.62	92.6	0.102
107.8 ± 0.75	103.1	102.9	0.209
156.4	149.3	···	···
162.1 ± 1.3	155.0	154.	0.166
186.5	179.1	179.	0.062
198.0 ± 1.8	190.0	192.0	0.557
			Total 1.481
	$J = \frac{1}{2}^-$		
···	···	12.6	0.040
47.4 ± 0.22	45.0	45.0	0.166
56.9 ± 0.29	54.1	53.9	0.092
111.3 ± 1.0	106.3	106.0	0.419
136.5 ± 1.4	130.5	129.5	0.256
139.6 ± 1.4	133.5	132.5	0.314
No data		141.6	0.148
No data		159.0	0.216
			Total 1.651
	$J = \frac{3}{2}^-$		
23.8 ± 0.1	22.4	22.0	0.020
32.9 ± 0.1	31.1	31.0	0.018
51.5 ± 0.3	48.9	48.8	0.034
under strong s-wave level		62.0	0.189
84.7 ± 0.6	80.7	81.4	0.093
120.6 ± 1.1	115.2	114.8	0.205
···	···	162.0	0.231
···	···	187.0	0.165
			Total 1.067
	Unassigned levels		
93.3	89.0	89.0	0.014
···	···	107.9	0.032
No data		175.0	0.067
			Total 0.113

able from capture measurements are limited in amount and precision, but they suggest that $\Gamma_n/\Gamma \approx 1$ above 100 keV. The values of the neutron p-wave strength function S_1 observed for these targets[18] also support this conclusion. The average neutron width at 100 keV inferred from the value of S_1 for ^{53}Cr is an order of magnitude larger than Γ_γ. In view of these facts, we can improve the reliability of estimates of $\Gamma_{\gamma 0}$ for negative-parity levels or p-wave resonances by restricting the analysis to energies above 100 keV. This convention was observed in the determination of radiative strengths (Sec. IV A).

A. $E1$ and $M1$ Radiative Strengths

The results for the integrated strengths and reduced widths of $E1$ and $M1$ radiative transitions are summarized in Table VII. The quantity $\sum g\Gamma_{\gamma 0}\Gamma_n/\Gamma$ is presented as a measure of the relative intensities of the various spin and parity components in the photoneutron spectra. The reduced width for electric dipole transitions was calculated from the expression

$$\bar{k}_{E1} = \sum \Gamma_{\gamma 0}/E_\gamma{}^3 A^{2/3}\Delta E ,$$

while the corresponding quantity used for magnetic dipole transitions was

$$\bar{k}_{M1} = \sum \Gamma_{\gamma 0}/E_\gamma{}^3 \Delta E ,$$

where $\bar{k}$ is the average reduced width and ΔE is the energy interval in which resonances used in the analysis were found. $\Gamma_{\gamma 0}$ is in eV; ΔE and E_γ are in MeV.

As defined above, the reduced widths would be the same for all nuclei if transitions could be described in terms of the single-particle model of the radiative process. These estimates are known to be only crude approximations to the actual situation. From $E1$ thermal-neutron capture γ rays, Bartholomew[23] has estimated $\bar{k}_{E1}\times 10^3 = 3.2$, while the results of Carpenter[24] for resonance γ rays indicate $\bar{k}_{E1}\times 10^3 = 3.7$. The results of this experiment give $\bar{k}_{E1}\times 10^3 = 1.7$ for ^{53}Cr, $\bar{k}_{E1}\times 10^3 = 0.9$ for ^{57}Fe, and $\bar{k}_{E1}\times 10^3 = 1.0$ for ^{61}Ni – all substantially lower than the single-particle estimates. An alternative relationship is based on the behavior of the tail of the giant dipole resonance in the excitation region near the neutron binding energy. Axel[25] has applied detailed balance to estimate the electric dipole photon strength function. The relation he obtained is

$$\bar{\Gamma}/D = (6.1\times 10^{-15})E^5 A^{8/3} .$$

In terms of the reduced width this would be

$$\bar{k}_{E1} = (6.1\times 10^{-9})E^2 A^2 ,$$

and for the nuclei studied here this would yield a value $\bar{k}_{E1}\times 10^3 = 1.2$ – in substantially improved agreement with observation. However, it should be noted that studies[24] of heavy nuclei imply that the above relation overestimates the reduced widths by as much as a factor of 2. Consequently, the "giant-resonance" estimate must be regarded as only approximate in spite of the apparent agreement observed here.

The group at Livermore has reported results[6] of threshold photoneutron measurements on ^{53}Cr and ^{57}Fe. Although they did not observe angular distri-

TABLE VII. Integrated yields and reduced widths for electric and magnetic dipole radiation. Integrated yields are given for all resonances observed, but reduced widths for magnetic dipole transitions are calculated only from yields for p-wave levels above 100-keV neutron energy (see discussion in Sec. IV). The number of resonance widths used to obtain each $\bar{k}$ is given by n. The errors given were calculated by assuming that the individual $\Gamma_{\gamma 0}$'s follow a Porter-Thomas distribution.

Target	J^π	$\sum g\,\Gamma_{\gamma 0}\Gamma_n/\Gamma$ (eV)	$\sum \Gamma_{\gamma 0}\Gamma_n/\Gamma$ (eV)	n	$10^3\times$ reduced width Individual average	
^{53}Cr	$\frac{1}{2}^+$	0.97	3.88	7	$\bar{k}_{E1} = 1.7^{+1.7}_{-0.5}$	
	$\frac{1}{2}^-$	1.27	5.06	6	$\bar{k}_{M1} = 41$	$\bar{k}_{M1} = 28^{+15}_{-8}$
	$\frac{3}{2}^-$	0.86	1.71	10	$\bar{k}_{M1} = 16$	
^{57}Fe	$\frac{1}{2}^+$	0.83	1.66	8	$\bar{k}_{E1} = 0.86^{+0.8}_{-0.3}$	
	$\frac{1}{2}^-$	0.37	0.74	4	$\bar{k}_{M1} = 9$	$\bar{k}_{M1} = 10^{+10}_{-3}$
	$\frac{3}{2}^-$	0.84	0.84	3	$\bar{k}_{M1} = 10$	
^{61}Ni	$\frac{1}{2}^+$	0.37	1.48	11	$\bar{k}_{E1} = 0.96^{+0.42}_{-0.19}$	
	$\frac{1}{2}^-$	0.41	1.65	5	$\bar{k}_{M1} = 27$	$\bar{k}_{M1} = 20^{+18}_{-7}$
	$\frac{3}{2}^-$	0.54	1.07	3	$\bar{k}_{M1} = 12$	

butions, they identified $\frac{1}{2}^+$ levels by comparison with the total neutron cross sections for ^{52}Cr and ^{56}Fe. Their results for the radiative strength of $E1$ transitions are stated in terms of the photon strength function $\langle \Gamma_{\gamma 0} \rangle / \bar{D}$. The value 1.2×10^{-5} inferred from our ^{53}Cr data agrees with their reported value if the latter is corrected to correspond to the recently revised value $g(n,\gamma)\Gamma_{\gamma 0} = 3.18$ eV for the normalizing resonance in ^{208}Pb. For ^{57}Fe we observe a value 0.6×10^{-5} compared to the corrected Livermore value of 0.8×10^{-5}. However, the discrepancy arises from our assignment of $J = \frac{3}{2}^-$ to an intense resonance at 235 keV as a result of the large observed anisotropy for that neutron group. Apparently a p-wave level strongly excited in (γ, n) reactions occurs near the expected position for a $\frac{1}{2}^+$ level.

In order to eliminate the influence of the neutron branching ratio Γ_n/Γ, the reduced widths for $M1$ transitions were calculated from the resonance structure above 100 keV. The values $\bar{k}_{M1}$ calculated for each possible p-wave spin are included in Table VII; but, in view of the limited precision of these values, the discussion is focused on the value of $\bar{k}_{M1}$ obtained for each nucleus by averaging the values observed for the two spins. The errors were calculated on the basis of the number of resonances actually observed and under the assumption that individual widths are governed by the Porter-Thomas distribution. The reduced widths observed for the three targets are statistically consistent with a single value $\bar{k}_{M1}$ equal to the observed average $\bar{k}_{M1} = 19 \times 10^{-3}$.

The available data on reduced widths for $M1$ transitions were summarized recently by Bollinger.[3] The essential conclusion of the survey is that,

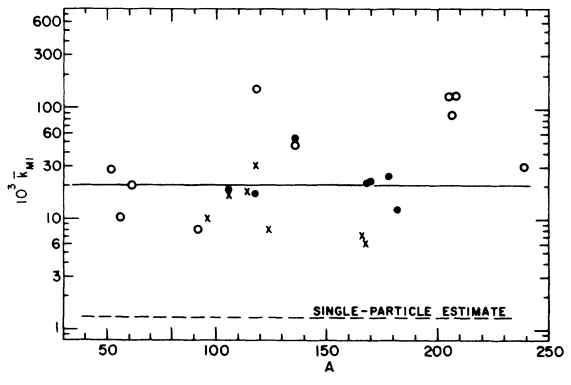

FIG. 8. Summary of reduced widths for $M1$ transitions, taken in part from Ref. 3. ×'s result from studies of capture of thermal neutrons, open circles from studies of neutron resonances, and solid circles from observations of average capture spectra. The errors in individual points are typically about a factor of 2.

with certain exceptions, the data on nuclei in the range $A = 80$–250 are consistent with $\bar{k}_{M1} \approx 20 \times 10^{-3}$. Results for ^{117}Sn, ^{119}Sn, ^{138}Ba, and ^{208}Pb suggest that the $M1$ strength may be enhanced in these closed-shell nuclei. The data are shown in Fig. 8. The strong enhancement of the reduced width in all nuclei over the single-particle estimate is generally accepted. With the addition of our results for ^{53}Cr, ^{57}Fe, and ^{61}Ni, the region in which $\bar{k}_{M1}$ can be crudely described by $\bar{k}_{M1} \approx 20 \times 10^{-3}$ is extended down to $A \approx 50$.

Although no published theoretical efforts account in any systematic way for the observed behavior of $\bar{k}_{M1}$, nuclear-structure effects that cause radiative strength to vary rapidly with photon energy and atomic mass were predicted originally by Mottelson[8] on the basis of very general considerations. The basic feature of these predictions is an enhancement of radiative strength for states in regions of excitation containing strong two-quasiparticle excitations of the appropriate character. For $M1$ transitions, these excitations are those generated by spin-flip transitions between the subshells of a given shell-model orbital split by spin-orbit coupling, viz. $(g_{9/2})^{-1}(g_{7/2})$. The targets used in our measurements were chosen because of their proximity to the $N = 28$ nucleon shell, which closes at the $f_{7/2}$ shell-model level. Calculations of energy eigenvalues above the Fermi energy in a Woods-Saxon potential[26] show that near $A = 50$ the energy difference between the filled $1f_{7/2}$ level and the empty $1f_{5/2}$ orbital is about 8 MeV, quite close to the excitation energies studied in this experiment. On this basis one might have expected a strong enhancement of $M1$ strength for nuclei near the $N = 28$ shell, but our results indicate that such is not the case.

B. Anomalous Concentrations of Radiative Strength

A point of considerable interest is the extent to which the observed distribution of radiative strength among resonances deviates from that expected for a statistically complex nucleus. In the latter case the widths should have a Porter-Thomas distribution, and the spacings the usual Wigner distribution. Sharp concentrations of strength in resonances in a small energy interval represent clear departures from the usual statistical picture, and can be interpreted as evidence for doorway states[27] if the spins and parities of the levels correspond to simple excited-state configurations of the target.

In the earlier studies of the (γ, n) reactions on ^{53}Cr and ^{57}Fe, the Livermore group proposed three candidates[28] for such possible doorway

states: groups of levels at 100 keV in ^{53}Cr and at 50 and 250 keV in ^{57}Fe. These anomalous concentrations of strength (i.e., "photon doorways") are not observed in our data, and a detailed comparison of the locations of individual resonances observed in the two experiments shows very poor agreement. For example, of the 29 resonances reported in ^{53}Cr below 333 keV, we observe only 21 and we also find four resonances not reported earlier. In ^{57}Fe we observe only 18 of 26 levels reported. In the energy interval 30–70 keV, in which a possible $\frac{3}{2}^+$ doorway state was proposed, we observe only three of the seven levels reported. Since the yields indicated for these seven levels were all equal within a factor of 2, the discrepancy cannot be explained on the basis of a possible inadequate sensitivity in our experiment. However, as Baglan, Bowman, and Berman[6] indicate, their spectra were obtained with bremsstrahlung whose end-point energy was sufficiently high above the threshold that the resonance structure included many neutron groups corresponding to decay to excited states of the daughter nuclei. The discrepancies between the two experiments most likely result from this fact, and provide a convincing example of the necessity of satisfying the photoneutron threshold condition when using bremsstrahlung in this type of study.

From a detailed examination of our data, we have concluded that no substantial evidence exists for the photon doorways in ^{53}Cr and ^{57}Fe at the energies proposed by the Livermore group. In the case of the candidate in ^{53}Cr near 100 keV, a cluster of five $J=\frac{3}{2}^-$ levels is observed between 100 and 133 keV, but the total radiative strength of the cluster obtained from our data is less than $\frac{1}{2}$ of the reported value.[6] To test the hypothesis that the observed clustering might be a simple statistical fluctuation in a population of levels obeying the Wigner distribution for level spacings and the Porter-Thomas distribution for $\Gamma_{\gamma 0}$, a Monte Carlo calculation was performed. Clustering in excess of that observed in this experiment was observed 16% of the time. In our judgment, this frequency is so high as to eliminate the photoneutron spectrum as evidence for a photon doorway. In the photoneutron spectra of ^{57}Fe we observe only three of the seven levels reported between 30 and 70 keV which were assumed to constitute a $\frac{3}{2}^+$ doorway; and among those resonances proposed as a $\frac{1}{2}^+$ doorway centered at about 250 keV we find one of the strongest, the one at 232 keV, should be assigned a spin and parity of $\frac{3}{2}^-$. In view of these observations our conclusion is that the photoneutron data do not give a statistically significant indication of those photon doorways proposed by Baglan.[28]

However, the concentration of strength which we observe in ^{57}Fe in the $\frac{3}{2}^-$ doublet at about 230 keV is clearly inconsistent with a statistical distribution of radiative strength. As suggested by the discussion in Sec. IV A this effect can be attributed to the presence in the excited-state wave function of a large admixture of the configuration of a $f_{5/2}f_{7/2}^{-1}$ particle-hole coupled to the ^{57}Fe ground state. This situation is at variance with the usual assumption of wave functions of extreme complexity and random character used to justify the Porter-Thomas distribution. But, it should be noted that the proposed single-particle state is not a doorway state in the frequently construed sense of being a 2p-1h system that can be excited in a simple way by the interaction of a neutron with a ^{56}Fe target. Hamamoto and Arima[29] have studied the composition of the ground state of ^{57}Fe and none of the states formed by coupling their configurations to $f_{5/2}f_{7/2}^{-1}$ could decay directly to ^{56}Fe$+n$ by particle-hole annihilation and emission of a $p_{3/2}$ neutron. In the current doorway terminology, our proposed particle-hole ^{57}Fe-core configuration would be described as a simple $\frac{3}{2}^-$ doorway in the photon channel but would not be a "common" doorway also present in the neutron channel. The fact that the configuration is not connected in any simple way with the neutron channel does not inhibit the (γ,n) reaction, because the neutron

TABLE VIII. Correlation coefficients $\rho_{\text{obs}}(\Gamma_n^0, \Gamma_{\gamma 0})$ between reduced neutron widths and ground-state radiation widths for levels in ^{53}Cr, ^{57}Fe, and ^{61}Ni which decay by emission of s-wave neutrons. The column at the right gives the probability that a population of uncorrelated pairs will give a value ρ' larger than the observed value ρ_{obs}. The values used for Γ_n^0 were taken from References 18 and 22. The sample labeled "total" was obtained by combining all pairs (Γ_n^0, $\Gamma_{\gamma 0}$) without regard to nucleus and using the resulting mean values of Γ_n^0 and $\Gamma_{\gamma 0}$ in the analysis.

Nucleus	Number of resonances	$\rho_{\text{obs}}(\Gamma_n^0, \Gamma_{\gamma 0})$	$P_{\rho=0}(\rho' > \rho_{\text{obs}})$
^{53}Cr	7	0.037	0.47
^{57}Fe	9	0.106	0.39
^{61}Ni	12	0.393	0.10
Total	28	0.071	0.35

channel is virtually the only channel open ($\Gamma_n/\Gamma \approx 1$ even for Γ_n very much less than the single-particle estimate).

C. Correlations Between Γ_n^0 and $\Gamma_{\gamma 0}$

Block, Stieglitz, and Hockenbury (BSH)[30] have recently reported evidence for a strong correlation between the reduced neutron width $\Gamma_n{}^0$ and the total radiation width Γ_γ for even-even target nuclei in the mass range $A = 50-60$. Because the capture spectra are dominated by strong high-energy transitions, they suggest that the observed effect arises from the existence of positive correlations between the neutron width and the partial radiation widths for these transitions. The compound states involved are also excited in the photoneutron experiments by absorption of electric dipole radiation. If the correlation suggested exists for the ground-state transitions, it should be evident in the results of this experiment. We tested for such an effect by examining the data for a correlation between the reduced neutron widths for s-wave resonances in the compound nuclei ^{53}Cr, ^{57}Fe, and ^{61}Ni and the corresponding ground-state radiation widths observed in this experiment. The results are shown in Table VIII, where the observed correlation coefficient ρ_{obs} between the variables $\Gamma_n{}^0$ and $\Gamma_{\gamma 0}$ are tabulated for s-wave resonances in each target studied and for the total population of s-wave levels in all three targets. The probability of obtaining a value of ρ larger than ρ_{obs} from a population with $\rho_{true} = 0$ is also given. In none of the cases is there evidence for a strong correlation; only for ^{61}Ni do the data suggest the possible existence of a weak effect. These values of ρ_{obs} are to be compared with the value 0.80 observed by BSH for 12 s-wave resonances in ^{51}Cr, ^{53}Cr, ^{55}Cr, and ^{61}Ni, which indicates with a 99% confidence limit that a significant effect exists. In the targets we have studied, it appears that the strong correlation BSH observed between Γ_γ and $\Gamma_n{}^0$ cannot be attributed to the ground-state transition.

Because the values of the reduced neutron widths for p-wave resonances have not been measured, we were unable to perform a correlation analysis for these levels.

ACKNOWLEDGMENTS

It is pleasure to thank L. M. Bollinger for his encouragement and support and D. Kurath for several discussions concerning the results reported here. The authors also gratefully acknowledge the support of K. Johnson, G. Mavrogenes, and W. Ramler who are responsible in large measure for the exceptional design of the Argonne National Laboratory linear accelerator, the linac operations group under L. Rawson for the excellent accelerator performance, and J. Specht for his continuing efforts in the design and fabrication of the neutron detector system.

---

*Work performed under the auspices of the U. S. Atomic Energy Commission.

†Permanent address: Macalester College, St. Paul, Minnesota 55105.

[1]L. M. Bollinger and G. E. Thomas, Phys. Rev. Letters 18, 1143 (1967); Phys. Rev. C 2, 1951 (1970).

[2]G. A. Bartholomew, in *Proceedings of the International Symposium on Neutron-Capture Gamma-Ray Spectroscopy, Studsvik, Sweden, August 1969* (International Atomic Energy Agency, Vienna, Austria, 1969), p. 553.

[3]L. M. Bollinger, in *International Symposium on Nuclear Structure, Dubna, 1968* (International Atomic Energy Agency, Vienna, Austria, 1969), p. 317.

[4]W. Bertozzi, C. P. Sargent, and W. Turchinetz, Phys. Rev. Letters 6, 108 (1963).

[5]C. P. Sargent, W. Bertozzi, P. Demos, and W. Turchinetz, in *Neutron Time-of-Flight Methods* (European Atomic Energy Community, Brussels, Belgium, 1961), p. 353.

[6]R. J. Baglan, C. D. Bowman, and B. L. Berman, Phys. Rev. C 3, 679 (1971), and references contained therein.

[7]L. M. Bollinger, Atomic Energy Commission Report No. CONF 660303 (U. S. GPO, Washington, D. C., 1966), p. 1064.

[8]B. R. Mottleson, in *Proceedings of the International Conference on Nuclear Structure, Kingston, 1960,* edited by D. A. Bromley and E. W. Vogt (University of Toronto Press, Toronto, Canada, 1960), p. 525.

[9]D. M. Brink, Argonne National Laboratory Report No. ANL-6796, 1963 (unpublished), p. 194.

[10]For a discussion of relevant aspects of angular correlations see L. C. Biedenharn, in *Nuclear Spectroscopy,* edited by F. Ajzenberg-Selove (Academic, New York, 1960), Pt. B, p. 732.

[11]W. Gallagher, K. Johnson, G. Mavrogenes, and W. Ramler, IEEE Trans. Nucl. Sci. 18, 584 (1971).

[12]M. J. Berger and S. M. Seltzer, Phys. Rev. C 2, 621 (1970).

[13]A. A. O'Dell, Jr., C. W. Sandifer, R. B. Knowlen, and W. D. George, Nucl. Instr. Methods 61, 340 (1968).

[14]J. A. Biggerstaff, J. R. Bird, J. H. Gibbons, and W. M. Good, Phys. Rev. 154, 1136 (1966).

[15]B. J. Allen and R. L. Macklin, Phys. Rev. Letters 25, 1675 (1970); and to be published.

[16]Available from National Neutron Cross Section Center, Brookhaven National Laboratory, Upton, New York.

[17]E. R. Rae, in Symposium on Neutron Standards and Flux Normalizations, Argonne National Laboratory, 1970 (unpublished).

[18]R. G. Stieglitz, R. W. Hockenbury, and R. C. Block,

Nucl. Phys. A163, 592 (1971).
[19]C. D. Bowman, E. G. Bilpuch, and H. W. Newson, Ann. Phys. (N.Y.) 17, 319 (1962).
[20]H. W. Newson, in *Nuclear Structure with Neutrons*, edited by M. Néve de Mévergnies, P. Van Assche, and J. Vervier (North-Holland, Amsterdam, 1965), p. 195.
[21]D. H. Wilkinson, in Ref. 10, p. 852.
[22]R. W. Hockenbury, L. M. Bartolome, J. R. Tatarczuk, W. R. Moyer, and R. C. Block, Phys. Rev. 178, 1746 (1969).
[23]G. A. Bartholomew, Ann. Rev. Nucl. Sci. 11, 259 (1961).
[24]R. T. Carpenter, Argonne National Laboratory Report No. ANL-6589, 1962 (unpublished).
[25]P. Axel, Phys. Rev. 126, 671 (1962).
[26]J. E. Lynn, *The Theory of Neutron Resonance Reactions* (Clarendon Press, Oxford, 1968), p. 103.
[27]H. Feshbach, A. K. Kerman, and R. H. Lemmer, Ann. Phys. (N.Y.) 41, 230 (1967).
[28]R. J. Baglan, C. D. Bowman, and B. L. Berman, Bull. Am. Phys. Soc. 15, 481 (1970); Phys. Rev. C 3, 2475 (1971).
[29]I. Hamamoto and A. Arima, Nucl. Phys. 37, 457 (1962).
[30]R. C. Block, R. G. Stieglitz, and R. W. Hockenbury, in Proceedings of the Third Neutron Cross-Section and Technology Conference, Knoxville, Tennessee, March 1970 (to be published).